Novel Method for Realizing 1000+ Electrode Array in Epi- or Subretinal Prosthesis

Diego Luján Villarreal, Dietmar Schroeder, and Wolfgang H. Krautschneider
Institute of Nano and Medical Electronics, Hamburg University of Technology, Hamburg, Germany
Email: {diego.lujan, d-schroeder, krautschneider}@tuhh.de

***Abstract*—From theoretical modelling, it is projected that a retinal device with 1000+ electrodes could provide face recognition, reading ability and functional vision. This challenging purpose, however, has a restriction to realize the boundaries of electrode carrier area with its corresponding electrode diameter to accommodate 1000+ microelectrodes and safeguard charge density, temperature increase at the device, and provide focal retinal stimulation, i.e. one active electrode excites a single cell. Here we introduce the strength electrode-separation curve and 'optimization window of epi- or subretinal stimulation' that answer the previously stated challenges. Further, a large-scale cell simulation is presented, which is a technique to obtain the optimal inter-electrode distance in epi- or subretinal stimulation.**

***Index Terms*—1000 electrode array retinal prosthesis, strength-duration curve, electrode carrier dimension limit**

I. Introduction

Epi- and sub retinal prosthetic devices have struggled for several decades to partially restore vision to those suffering retinal degenerative diseases such as Age-related Macular Degeneration (AMD) and Retinitis Pigmentosa (RP).

Although there have been noteworthy developments in this field, new devices may face additional challenges for safe micro electrode implantation.

From theoretical modelling, it is estimated that a 1000+ electrode device could provide a decent functional vision, i.e. reading ability, object and face recognition [1].

In [2], we learned that is feasible to stimulate safely ganglion cells with the following requirements: i) 1024 electrode array attaching 16 scalable chips of 64 electrodes each with a daisy chain configuration as seen in [3]; ii) reduce electrode diameter to 14 μm; iii) use maximum output voltage of 1 V; iv) pulse duration of 100 μs required to replicate light-elicited spiking patterns in individual ganglion cells; v) PEDOT-NaPSS electrode deposition; vi) inter electrode-ganglion cell distance I_{EGD}, less than 100 μm; vi) circular electrodes and vii) inter-electrode distance, I_{ED}, of 100 μm.

I_{ED}, however, plays a major role to trigger action potential in the ganglion cell, because it influences the depth of the current flow. When I_{ED} decreases, the current density passes superficially through the tissues. Vice versa, when I_{ED} increases the current density penetrates deeper into the tissues [4] and thus elicits activity in distal ganglion cells, thereby greatly reduce resolution [5].

In this work, we present a novel method to realize 1000+ electrode array using the strength electrode-separation curve and the 'optimization window of epiretinal stimulation' that provide useful guidance to i) find the boundaries of electrode carrier area to accommodate 1000+ electrodes; ii) be within the safe limits of charge density and heat increase at the device, iii) provide focal stimulation at the ganglion cell. Our model has the following characteristics:

i) 1024 electrode feasibility study.

ii) Focal stimulation.

iii) 100 μs pulse duration which is required to replicate light-elicited spiking patterns in individual ganglion cells [6].

iv) PEDOT-NaPSS arranged electrode array, where the active is surrounded by eight ground electrodes [2], to stress the isolation of the active electrode, to confine the stimulus current to a small volume around the ganglion cell and to minimize electrode cross-talk.

v) Maximum voltage of operation study.

vi) Charge density, focal stimulation and heat increase limitations.

vii) Circular electrodes to reduce elevated charge densities arising from irregular shapes [6].

viii) We used the exact simulation procedure and assumptions as seen in [2].

II. Methods

A. Strength Electrode-Separation Curve

The strength electrode-separation curve, S_{eSC}, shows the interdependence between the stimulus strength and the inter electrode distance required for ganglion cell activation.

Unlike to the well-known strength-duration curve, S_{DC}, which progressively activates more individual nerve fibers as the stimulus strength increases, the S_{eSC}, however, emphasizes the eliciting of a single ganglion cell as the stimulus strength increases at lower I_{ED}, thereby improving focal stimulation and greatly increase resolution.

The S_{eSC}, see Fig. 1, can give a graphic representation as to how electrodes must assemble in an electrode carrier for a given stimulus and I_{ED}. Ganglion cell relative excitability can be as well analyzed.

Manuscript received February 14, 2016; revised July 5, 2016.

doi: 10.18178/ijpmbs.5.3.146-153

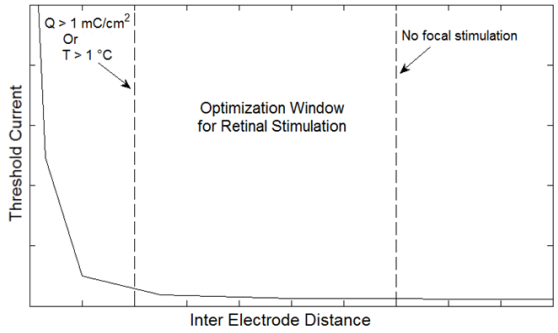

Figure 1. Strength electrode-separation curve with optimization window.

B. Optimization Window

The optimization window is the area between the limits of charge density and/or temperature increase at the device and the limit of focal retinal stimulation that can ensure safe operation.

The basic purpose of the optimization window is to find, with a known electrode diameter, the limits of safe I_{ED} and therefore the boundaries of minimum and maximum electrode carrier area that can support a 1000+ electrode array and be within safe stimulus deliver.

C. Ganglion Cell Model

Ganglion cell model has a basic mathematical structure for voltage-gating based on Hodgkin and Huxley like equations [7] and is modelled with an equivalent circuit taken from previously published model of repetitive firing of retinal ganglion cells [8]. The parameters and equations that describe the dynamics of the ionic channels were kept as in the original model

D. Retinal Model

We used the identical COMSOL model of the retina as seen in [2] with the variation of inter-electrode distance and polyimide carrier dimensions as is required in our study. The model is shown in Fig. 2.

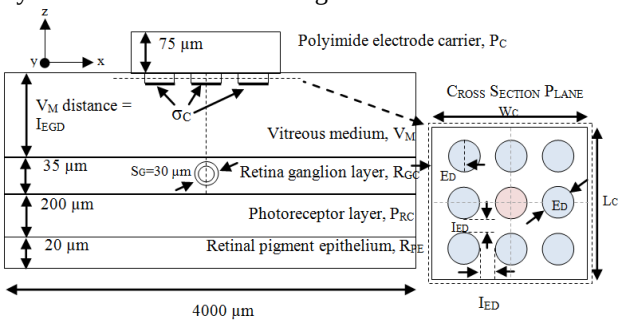

Figure 2. Retina model at COMSOL simulations. Layer thickness not drawn to scale.

It consists of seven domains: polyimide carrier of electrodes P_C; vitreous medium V_M; retina ganglion cell layer R_{GC}; photoreceptor layer P_{RC}; retinal pigment epithelium R_{PE}; ganglion cell soma S_G and the electrode array E_{ELE}. The ganglion cell soma was placed inside the retina ganglion cell layer exactly below the center of active electrode and was enclosed with the cell membrane. The material of the electrode is PEDOT-NaPSS electrodeposited in gold electrodes with a charge density of 40mC/cm^2 [9].

The electrode array configuration is shown at the cross section plane in the COMSOL model. This arrangement is analogous to [10], [11], however it consists of an active electrode (in red) surrounded by eight guards (in blue) in order to stress the isolation of the active electrode, to confine the stimulus current to a small volume around the ganglion cell and to minimize electrode cross-talk during stimulation.

E. Boundaries of Inter-Ganglion Cell Distance

Ganglion cell density, ρ_{GC}, is usually estimated as a function of eccentricity from the fovea. ρ_{GC} has a symmetric "bell curve" shape or Gaussian profile where the position of the center of the peak is around 1 °.

When safe navigation is required in dynamic out-door environments, stimulation should include eccentricities of 10–15 ° [12]. Curcio [13] has provided densities of 504 and 1634 cells/mm^2 for temporal and nasal coordinates, respectively, of young retinas at eccentricity of 10 °.

For estimating the ganglion cell density at electrode array location, we averaged the ganglion cell density at both coordinates, having a ρ_{GC} of 1073 cells/mm^2, considering a plausible electrode array displacement after implantation. The morphological bases that demonstrate the feasibility of the retinal implant indicated that 25% to 30% of ganglion cell are preserved in the inner retinal region in patients with AMD and RP [14]. Using the remaining ganglion cell percentage of 25%, a severe RP or AMD patient has approximately 268 cells/mm^2 of ρ_{GC}.

We assumed to have a square grid cell distribution, see Fig. 3.

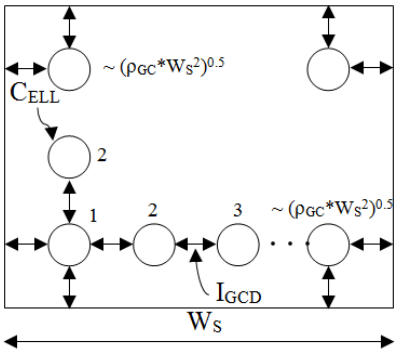

Figure 3. Square grid of ganglion cell distribution.

Using the square grid distribution with a ganglion cell diameter, d_{GC}, of 0.03 mm, we can compute the inter-ganglion cell distance IGCD, as follows:

$$I_{GCD} = \frac{W_S - (d_{GC} * \sqrt{\rho_{GC} * W_S^{\,2}})}{1 + \sqrt{\rho_{GC} * W_S^{\,2}}} \qquad (1)$$

For W_S of 1mm, the result is approx. 30 µm.

F. Boundaries of Inter-Electrode Distance

The maximum boundary of inter-electrode distance I_{EDMAX}, see Fig. 4, was defined as the maximum distance

of active and ground electrodes that achieves focal stimulation. Therefore, the current density must be contained in a small volume that surrounds the cell and ensures that each active electrode elicits activity in only one ganglion cell.

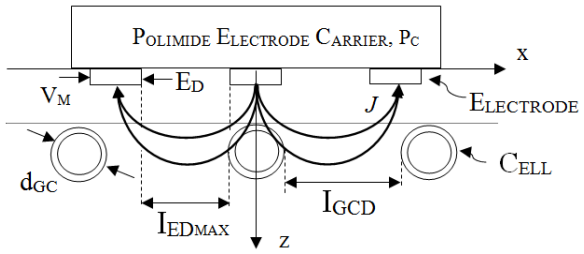

Figure 4. I_{EDMAX} illustration. All distances not drawn to scale.

I_{EDMAX} is calculated as follows:

$$I_{EDMax} = \frac{d_{GC}}{2} + I_{GCD} - E_D \quad (2)$$

Assuming that the center of active electrode is positioned at the origin, I_{EDMAX} starts when the tangents of active and ground electrodes meet.

G. Boundaries of Polymide Carrier

To achieve decent functional vision, i.e. reading ability, object and face recognition, it is required an array for implantation of 1000+ electrodes.

Thereby, to achieve this request, the width, W_{EC}, and length, L_{EC}, of polyimide carrier are calculated assuming an evenly electrode distribution

$$W_{EC} = L_{EC} = I_{ED} * (\sqrt{e_T} + 1) + E_D * \sqrt{e_T} \quad (3)$$

e_T is the total number of electrodes considered of 1024. I_{ED} is the edge-to-edge inter-electrode distance.

We can calculate the area of electrode carrier based on I_{ED} and E_D as $A_{EC} = W_{EC} * L_{EC}$.

H. Simulation Procedure – Ganglion Cell Model

In this work we used the identical ganglion cell model as [8] to calculate in Matlab the extracellular threshold current density of the ganglion cell with a modification on the pulse duration as is required in our study.

We used a monophasic rectangular pulse for electrical stimulation at the ganglion cell.

In our case we simulated the ganglion cell model only at 100 μs and applied at 500 pulses per second, taking into account absolute and refractory period of an action potential.

The peak current density amplitude was swept with a resolution of 1 μA/cm^2 until it was found the threshold current density that fires a train of action potential. The result of extracellular peak current amplitude is 120 μA/cm^2 for 100 μs.

I. Simulation Procedure – Retinal 3D Model

The retinal modelling was built using COMSOL Multiphysics. In this work we used the identical retinal model as [2]. The ganglion cell soma was placed inside the retina ganglion cell layer exactly below the center of active electrode and was enclosed with the cell membrane.

After obtaining the extracellular peak current amplitude in Matlab environment, that result was used to match the average boundary current density of the ganglion cell by applying current from the active electrode.

In this work, we varied I_{ED}, I_{EGD} and E_D, to plot the strength electrode-separation curve and to find the 'optimization window of retinal stimulation'. The I_{EGD} tested are 10, 50 and 100 μm. The E_D tested are 2, 5, 10, 15 μm. We simulated the retinal model until I_{ED} of 100 μm. All values are edge-to-edge inter electrode distances.

We iterated the retinal model for each I_{ED}, E_D and I_{EGD} until we obtained the threshold current flowing from the active electrode. Out of COMSOL simulations, we also obtained the voltage across the electrodes over time.

J. Charge Density Limit Calculation

The charge density was obtained by integrating the current delivered by the active electrode over time and dividing it by the electrode area. It is worth to mention that all eight surrounding electrodes including the active changed their dimensions accordingly.

As there is no evidence about safe gas-free and erosion-free operation charge densities on PEDOT-NaPSS low electrode area, we used the limit of 1 mC/cm^2 at the electrodes. We used a monophasic rectangular pulse for electrical stimulation at the ganglion cell.

We interpolated the data of charge density for each case to find the charge density limit that can ensure safe operation within the restriction of 1 mC/cm^2.

K. Temperature Limit and Output Voltage of Operation Calculation

Regarding the calculation of the power consumption and temperature increase at the device, we used the same approach to calculate the average power density of 1024 evenly distributed electrodes as seen in [2]. That means, the sum of the power of the transistors that drive the electrodes and the power consumed per Local Stimulation Unit is sufficient to describe the total average power density of the device.

We interpolated the data of temperature increase at the device for each case to find the temperature limit that can ensure safe operation within the boundary of 1 ℃.

The results of electrode potential were used as the maximum output voltage of operation while stimulating the retina. Then, we performed the same interpolation procedure with the voltage supply of 3.3V, and 1V as a condition boundary of the output voltage of operation.

For each case, we selected the I_{ED} limit of F_{S0} to be the boundary that can ensure safe operation within the restriction of 1mC/cm^2 and 1 ℃. F_{SX} is equal to I_{EDMAX}.

The difference between F_{SX} and F_{S0} determines the optimization window. When $F_{S0} > F_{Sx}$, however, the optimization window is closed because either the charge density of temperature limit was higher than the restrictions specified.

L. Large-Scale Ganglion Cell Simulation

The goal of large-scale simulation is to find the optimal I_{ED} within the optimization window. It is based on

conditions that ensure cell stimulation when the cell is not placed exactly below the center of active electrode.

1) Spatial condition of cell excitation

We approximated the fact that the percentage of stimulated cells decreases for larger distances from the electrode by assuming that all cells closer than the spatial condition or S_C are stimulated, while all cells of larger distances are not stimulated.

Using the same approach as in the COMSOL model, we shifted the ganglion cell along the 'x' coordinate in COMSOL simulation to calculate the boundary current density at the membrane, see Fig. 5.

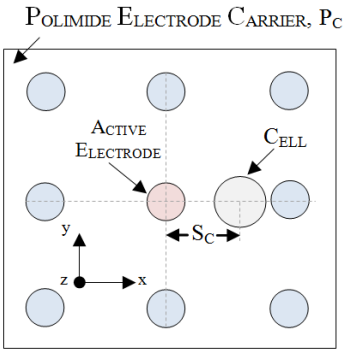

Figure 5. Spatial condition of cell excitation for all E_D.

After getting the boundary current at the membrane for each E_D and I_{ED}, we interpolated the data to find S_C.

The value of S_C was determined such that on average 85% of stimulation occurred within this distance, see Fig. 6.

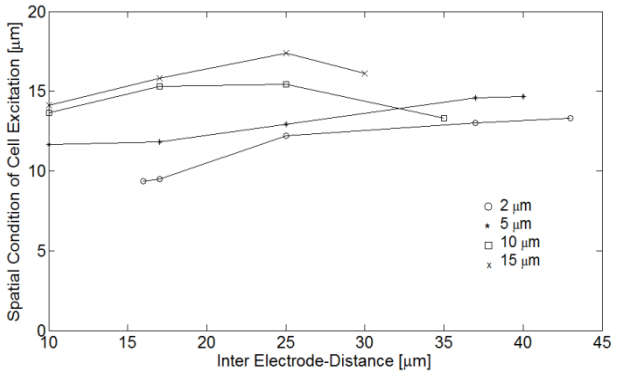

Figure 6. Spatial condition of cell excitation for all E_D.

We simulated from I_{ED} of 10 µm to I_{EDMAX} for the corresponding E_D. For E_D of 2 µm, however, we started at F_{S0}. We chose to cut down I_{ED} because: i) using low I_{ED} means less number of ganglion cells included, G_C, due to its dependence of electrode carrier area and ganglion cell density as $G_C = A_{EC} * \rho_{GC}$. The spatial condition also shows the maximum distance to excite a cell.

2) Large-Scale simulation procedure

Once realizing the optimization window for each case, we generated a Matlab script to describe a Large-Scale Simulation (LSS) of ganglion cell stimulation.

The Matlab script executed a group of statements in a loop to find whether the cell was stimulated based on S_C.

We produced a random distribution of cells on the area A_{EC}, such that the distances to the neighboring cell (or the edges) in each axis are uniformly distributed between 15 and 45 µm.

The overlapping ganglion cells, O_{GC}, were counted and were eliminated to avoid issues of an unreal case scenario.

The electrodes were evenly distributed along a defined matrix $E_{b,a}$ with dimensions of $1 \leqslant b \leqslant e_T^{0.5}$ and $1 \leqslant a \leqslant e_T^{0.5}$, where e_T is the total electrodes considered of 1024. Each electrode is separated with an inter electrode distance, I_{ED}.

In our simulations, we assumed i) to assemble the array of electrodes homogeneously in order to give the advantage to program each to function as an active or ground electrode; ii) we followed the same configuration as seen in [2]: each electrode can have a different timeslot and each can be activated independently with a total image frequency of 20Hz; and iii) we used the same approach of active-surrounding ground electrode configuration as seen in the COMSOL model.

III. Results

A. Strength Electrode-Separation Curve and Optimization Window

Fig. 7 to Fig. 10 illustrate the strength electrode-separation curve with the optimization window for I_{EGD} of 10, 50 and 100 µm in semilog-style for better representation.

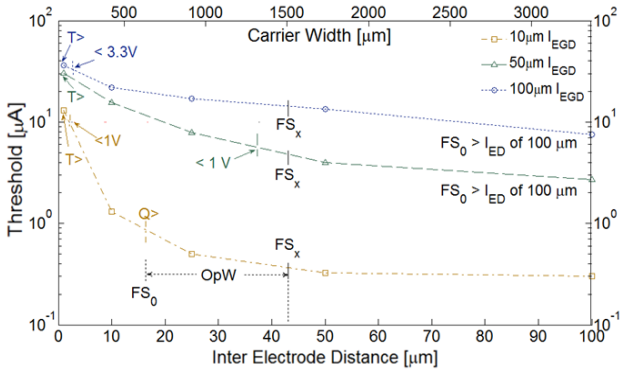

Figure 7. S_{esC} with optimization window for E_D of 2 µm.

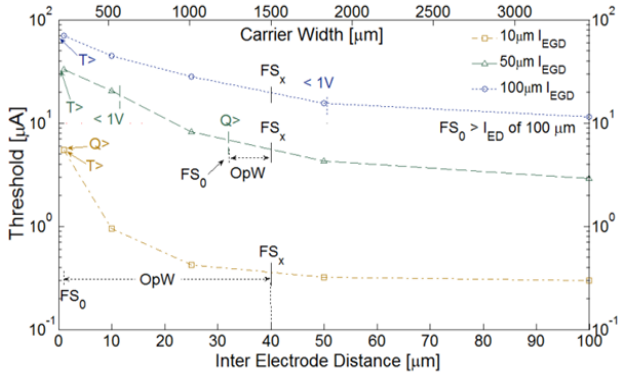

Figure 8. S_{esC} with optimization window for E_D of 5 µm.

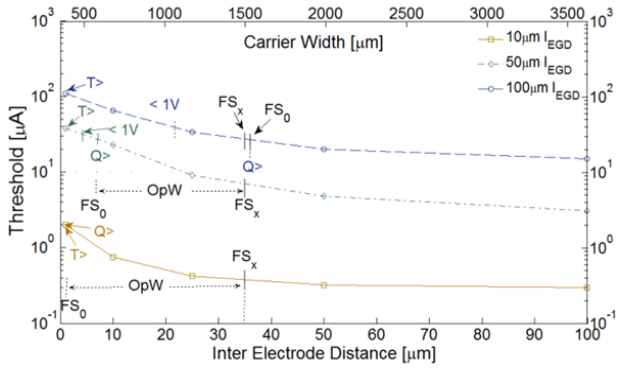

Figure 9. S_{eSC} with optimization window for E_D of 10 µm.

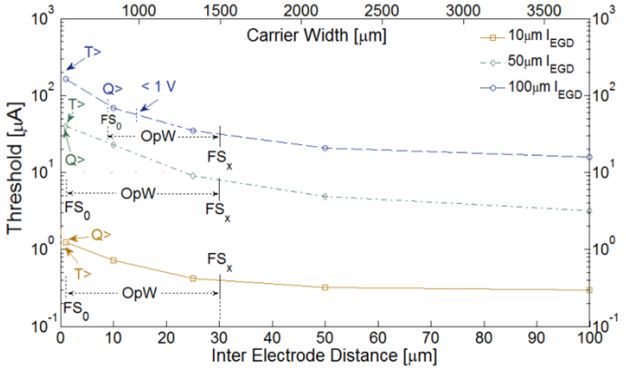

Figure 10. S_{eSC} with optimization window for E_D of 15 µm.

Each of them shows the results for a specific E_D with the safe limits of charge density, temperature increase at the device and maximum output voltage with respect of I_{ED}.

On top, the width of electrode carrier W_{EC} it is given. As a reminder, W_{EC} is equal to the electrode carrier length, L_{EC}. The carrier area is calculated as $A_{EC} = (W_{EC} * L_{EC})$. Each of the configurations has their own electrode carrier area.

B. Large-Scale Ganglion Cell

Out of the Matlab script, we obtained: i) the average effective stimulation, E_S, which is defined as the number of outcomes when a single ganglion cell is stimulated by a single active electrode, i.e. focal stimulation. We computed the percentage of effective stimulation as $100*E_S/e_T$; ii) average missed stimulation, M_S, which is defined as the number of outcomes when the active electrode did not stimulate any cell; iii) average ganglion cell activation, A_{GC}, which is defined as the number of outcomes when an active electrode stimulates a cell, regardless if it is stimulated focally or not. We computed the percentage of cell activation as $100*A_{GC}/(G_C-O_{GC})$; iv) average no-focal stimulation, N_{FS}, which is defined as the number of outcomes when an active electrode stimulates two or more cells.

Inside the Matlab script, we chose a step to have a total of 20 configurations. For each configuration, we repeated the simulation 150 times to produce a new random distribution of cells in order to attempt reaching an I_{GCD} real case randomness scenario and have meaningful conclusions about cell activation and electrode usage.

Then, we took the percentages explained above for each configuration and finally we averaged the results.

IV. Discussion

A. S_{eSC} and Optimization Window

The optimization window results are shown in the text box at Fig. 7 to Fig. 10 as 'OpW'.

As one might expect, a greater optimization window was observed at smaller I_{EGD} or greater E_D. This behavior can be attributed to the low electrode voltage and low charge density.

The results of the boundaries of electrode carrier area with respect to their electrode diameter are shown in Table I.

TABLE I. Boundaries of Electrode Carrier Area in (mm^2) with Respect of E_D in (µM). I_{EGD} Is the Inter-Electrode Ganglion Distance

	10 I_{EGD}		50 I_{EGD}		100 I_{EGD}	
E_D	From	I_{EDMAX}	From	I_{EDMAX}	From	I_{EDMAX}
2	0.38	2.25	-	-	-	-
5	0.04	2.19	1.48	2.19	-	-
10	0.12	2.18	0.40	2.18	-	-
15	0.26	2.16	0.26	2.16	0.64	2.16

The boundaries of minimum and maximum electrode carrier area are dependent on the technology limitations and they have their own advantages. Maximum carrier area provides a greater projected visual field assuming for every 1mm of the retina stimulated is about 3.35 °[15].

Minimum size area, however, provides an advantage to attach additional electrode carriers that will require low power circuit design. Moreover, decreasing electrode dimension will generate, however, higher resolution patterns of prosthetic-elicited activity that are closer to light-elicited patterns [16].

B. Charge Density Limits

The limits of charge density are shown in the text box at Fig. 7 to Fig. 10 as 'Q>', which represents the safe boundary under the corresponding I_{ED}.

As stated earlier, the charge density limit is $1mC/cm^2$. Our simulations agree with the tendency of charge density that increases once the E_D decreases and also because the lifting off of the electrode array from the retinal surface.

For E_D of 5 µm at I_{EGD} of 100 µm and E_D of 2 µm at I_{EGD} of 50 and 100 µm, the charge density limit was above I_{ED} of 100 µm and it was not shown as well as F_{S0}.

C. Threshold Current

As seen Fig. 7 to Fig. 10, for lower I_{ED} distances, i.e. lower than 50 µm, we observed that the threshold current becomes proportional to the square of I_{ED}.

Subsequently, for I_{ED} higher than 50 µm, the threshold changes are less pronounced. This behavior can be attributed to I_{ED} because it influences the depth of the current flow and plays a major role to trigger action potential in the ganglion cell. Threshold variations with respect to I_{EGD} are consistent with previous experimental work of epiretinal device implanted in rabbits [17].

D. Output Voltage of Operation

We used the voltage across the electrodes as the maximum output voltage of operation while stimulating the retina. Then, we compared it with the voltage supply of 3.3V, and 1V as a condition boundary of the output voltage of operation.

The limits are shown in the text box at Fig. 7 to Fig. 10 as '<1V' or '<3.3V', which indicates the boundary under the corresponding I_{ED}.

For the cases where any text box is shown, it represents that the results of electrode voltage were smaller than the <1V limit specified.

E. Focal Stimulation Limits

The limits of focal stimulation are indicated in Fig. 7 to Fig. 10 as F_{Sx}.

F. Temperature Increase at the Device

The limits of temperature at the device are shown in the text box at Fig. 7 to Fig. 10 as 'T>', which denotes the safe boundary under the corresponding I_{ED}. As stated earlier, the temperature limit is 1 ℃.

Regardless on E_D or I_{EGD}, our results show that the temperature does not play a major role on neural tissue heating from the retina prosthesis. This behavior can be attributed to the use of the duty cycle and few LSU per Δt explained thoroughly in [2].

G. LSS – Ganglion Cell Activation

Fig. 11 shows the average percentage results of electrode stimulation and ganglion cell activation versus I_{ED}. Note that the range of I_{ED} for each case corresponds to 10 µm I_{EGD}.

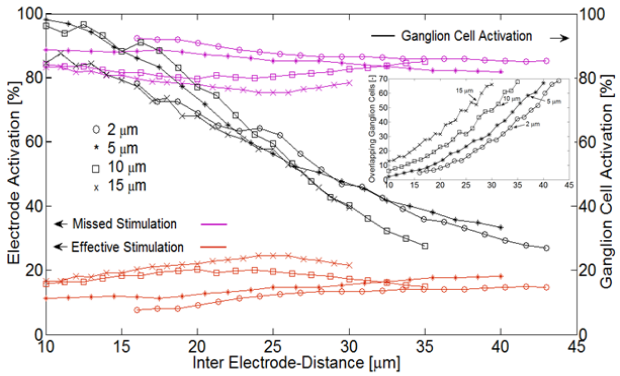

Figure 11. Large-Scale cell simulation results.

We chose to focus on 10 µm I_{EGD} to analyze the advantages to use different I_{ED}'s and E_D's on 1024 electrode array after surgery.

The aim of retinal prosthesis is not only to have a functional system of 1024 electrodes but also to activate, with focal stimulation, as many cells as possible in order to provide a decent functional vision, i.e. reading ability, object and face recognition.

Fig. 11 shows a trade-off between I_{ED} and the percentage of ganglion cell activation. Using $G_C = A_{EC} * \rho_{GC}$, when I_{ED} increases, G_C rises and as well A_{EC} as it becomes proportional to the square of I_{ED}. As A_{EC} increases, it gives a greater projected visual field assuming for every 1mm of the retina stimulated is about 3.35 °; however, the percentage of ganglion cell activation is reduced with an exponential decrease profile. As the I_{ED} becomes shorter, though, the electrodes are more concentrated on stimulating single cells, but G_C and the projected visual field are reduced.

Therefore, we investigated the ganglion cell activation A_{GC}, see Fig. 12.

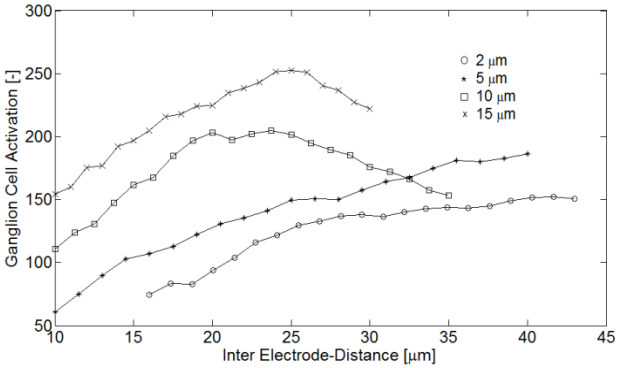

Figure 12. Ganglion cell activation.

We used the average of overlapping ganglion cells shown inside Fig. 11 to calculate the ganglion cell activation.

For all cases, the ganglion cell activation follows the profile of spatial condition of cell excitation. Each rose significantly from 10 µm I_{ED} because of the increase of G_C and A_{EC} as it develops proportional to the square of I_{ED}. Then, E_D of 10 and 15 µm reaches a peak at 24 and 25 µm. The final phase shows a rapid decrease in activation.

For E_D of 2 and 5 µm, however, the cell activation increased steadily, obeying the spatial condition of cell excitation. When looking for an I_{ED} for maximum ganglion cell activation, for 2, 5, 10 and 15 µm of E_D, the results are 42, 40, 24 and 25 µm of I_{ED} at 28, 33, 62, and 58 of % A_{GC}, all respectively.

A_{GC} results are 152, 186, 204 and 252 cells, all correspondingly. All optimal I_{ED} results were within the range of optimization window for their respective cases.

H. LSS – Electrode Utilization

As seen in Fig. 11, the effective stimulation, defined as the number of outcomes when a single ganglion cell is stimulated by a single active electrode, can be associated to the effective utilization of electrodes.

Fig. 13(A) and (B) show two examples of large scale simulation solved in Matlab.

Both plots, small dots, either red (effective stimulation E_S) or cyan (missed stimulation M_S) correspond to the electrodes. Large dots, either red (cell activation, A_{GC}) or cyan (not stimulated) correspond to ganglion cell.

Using Fig. 13(A) as an example, when the I_{ED} becomes smaller, G_C is reduced and the electrodes 'gather together' and are more concentrated on stimulating solitary ganglion cells. As the activation of ganglion cells increases, however, there exist groups of electrodes which do not collaborate on stimulating a cell. An unchanged situation but with different dimensions occurs when I_{ED} becomes higher (Fig. 13(B)).

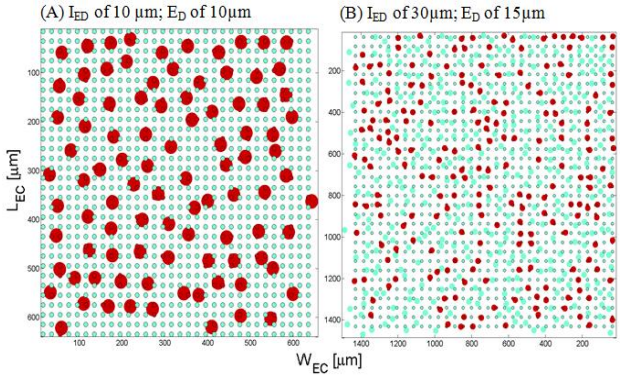

Figure 13. (A) and (B) examples of large-scale simulation.

The effective utilization of each electrode, Fig. 11, for all I_{ED} tested, remained fairly unchanged and followed strictly the spatial condition of cell excitation. The maximum of effective electrode usage are 15, 18, 20 and 25 % for E_D of 2, 5, 10 and 15 µm, all correspondingly.

The results of no-focal stimulation, N_{FS}, showed an average lower than one for all cases.

I. Spatial Condition of Cell Excitation

We noticed a variation in the spatial condition of cell stimulation when other current rather than the threshold was used.

The depth of penetration of the applied current has a dependency on the amplitude peak, which simultaneously defines the strength in the incoming current at a given geometrically shaped boundary. Using another current will cause irregularities in the spatial conditions of stimulation.

Therefore, it is imperative to use an accurate threshold current to compute the spatial condition of cell excitation.

V. Conclusion

In this work, we presented a novel method to find i) the boundaries of electrode carrier area with its corresponding electrode diameter to accommodate 1024 electrodes and safeguard charge density, temperature increase at the device and provide focal stimulation; and ii) the effective electrode usage and ganglion cell activation.

Assuming 1 ℃ and 1mC/cm^2 limit, our model suggests that is feasible to use a 1024 electrode array based on i) the maximum ganglion cell activation and ii) reducing electrode size which will generate higher resolution patterns of prosthetic-elicited activity that are closer to light-elicited patterns.

Nevertheless, we noticed a trade-off between reducing electrode diameter and increasing the effective electrode usage and ganglion cell activation.

For E_D of 2 µm, the maximum effective electrode usage is 15 % and stimulates around 152 cells. For E_D of 15 µm, however, the results rose to 25 % and 252 cells.

By stimulating with the right threshold current, each shows its own attributes:

i) E_D of 2 µm at I_{ED} of 42 µm has a greater projected visual field with 2.1mm^2 electrode array and generates higher resolution patterns.

ii) E_D of 15 µm at I_{ED} of 25 µm has higher effective electrode usage and ganglion cell activation. Each configuration works with 100 µs pulse duration, PEDOT-NaPSS electrode deposition and circular electrodes.

To avoid further issues caused by implantation of an epi-, sub-retinal or suprachoroidal implant, the inter electrode-ganglion cell distance plays a major role for a successful retina implant.

The major limitation, however, is attributed to the charge density required to elicit activity in neurons.

References

[1] G. Chader, J. Weiland, and M. S. Humayun, "Artificial vision: Needs, functioning, and testing of retinal electronic prosthesis," *Progress Brain Research*, vol. 175, pp. 317-332, 2009.
[2] D. L. Villarreal, *et al.*, "Feasibility study of a 1000+ electrode array in epiretinal prosthesis," presented at the 8th International Conference on Bioinformatics and Biomedical Technology. Barcelona, Spain, June 10-12, 2016.
[3] M. Meza-Cuevas, D Schroeder, and W. H. Krautschneider, "A scalable 64 channel neurostimulator based on a hybrid architecture of current steering DAC," in *Proc. Middle East Conference on Biomedical Engineering*, 2014.
[4] M. Radomski and C. A. T. Latham, *Occupational Therapy for Physical Dysfunction*, Lippincott Williams & Wilkins, 2008.
[5] P Tuppin, C Hiesse, Y Caillé, and M Kessler, "Differential responses to high-frequency electrical stimulation in ON and OFF retinal ganglion cells," *J. Neural Eng.*, vol. 11, pp. 517-524, 2014.
[6] S. Fried, H. A. Hsueh, and F. S. Werblin, "A method for generating precise temporal patterns of retinal spiking using prosthetic stimulation," *J. Neurophysiol*., vol. 95, pp. 970-978, 2006.
[7] A. Hodgkin and A. F. Huxley, "A quantitative description of membrane current and its application to conduction and excitation in nerve," *J. Physiol*., vol. 117, pp. 500-544, 1952.
[8] J. Fohlmeister, P. A. Coleman, and R. F. Miller, "Modeling the repetitive firing of retinal ganglion cells," *Brain Research*, vol. 510, pp. 343-345, 1989.
[9] R. Starbird, *et al.*, "Electrochemical properties of PEDOT-NaPSS galvanostatically deposited from an aqueous micellar media for invasive electrodes," in *Proc. IEEE BMEICON*, 2012.
[10] N. Lovell, S. Dokos, S. L. Cloherty, and P. J. Preston, "Current distribution during parallel stimulation: Implications for an epiretinal neuroprosthesis," *IEEE Eng. Med. Biol. Soc.*, vol. 5, no. 5, 2005.
[11] N. Dommel, *et al.*, "A CMOS retinal neurostimulator capable of focussed, simultaneous stimulation," *J. Neural Eng.*, vol. 6, p. 035006, 2009.
[12] R. Eckhorn, *et al.*, "Visual resolution with retinal implants estimated from recordings in cat visual cortex," *Vision Research*, vol. 46, no. 17, 2006.
[13] C. A. Curcio and K. A. Allen, "Topography of ganglion cells in human retina," *J. Comp. Neurol.*, vol. 300, no. 1, pp. 5-25, 1990.
[14] A. Santos, *et al.*, "Preservation of the inner retina in retinitis pigmentosa. A morphometric analysis," *Arch. Ophthalmol.*, vol. 115, pp. 511-515, 1997.
[15] L. Tychsen, "Binocular vision," in *Adler's Physiology of the Eye*, W. M. Hart, ed., St. Louis: Mosby Year Book, 1992.
[16] C. Cai, Q. Ren, N. J. Desai, and S. I. Fried, "Response variability to high rates of electric stimulation in retinal ganglion cells," *J. Neurophysiology*, vol. 106, pp. 153-162, 2011.
[17] R. J. Jensen and O. R. Ziv, "Thresholds for activation of rabbit retinal ganglion cells with relatively large, extracellular microelectrodes," *IOVS*, vol. 46, no. 4, 2005.

Diego Lujan Villarreal was born in Monterrey, Nuevo León, México in 1983. He received the B.S. degree in Mechatronics from the Monterrey Institute of Technology and Higher Education (ITESM) in 2006 and the M.S. degree in Microelectronics and Microsystems from the Hamburg University of Technology in 2010.

He has worked with the Cellular Therapy Department in the School of Medicine at ITESM, Monterrey, México, and he is now pursuing his PhD in the Institute of Nano and Medical Electronics at the Hamburg University of Technology, Hamburg, Germany. His main research interests focus on theoretical models of neurostimulation, optimal energy-saving algorithms and epi- and sub retinal stimulation.

Wolfgang H. Krautschneider (M'85) received the M.Sc., Ph.D., and Habilitation degrees from the Berlin University of Technology, Berlin, Germany. He was with Central Research Laboratories, IBM, Yorktown Heights, NY, USA, the Siemens Research Center, Munich, Germany, and the DRAM Project of IBM and Siemens, Essex Junction, VT, USA. He is currently the Head of the Institute of Nano and Medical Electronics at the Hamburg University of Technology, Hamburg, Germany.

Dietmar Schroeder (M'88–SM'94) received the Dr. Ing. degree in electrical engineering from the Technische Universität Braunschweig, Braunschweig, Germany, in 1984. He joined the Hamburg University of Technology, Hamburg, Germany, in 1983, where he has been a Lecturer with Semiconductor Electronics since 1994.